NACA RM No. L8L07

NACA

RESEARCH MEMORANDUM

ESTIMATION OF LIFT AND DRAG OF AIRFOILS AT NEAR SONIC SPEEDS AND IN THE PRESENCE OF DETACHED SHOCK WAVES

By

John P. Mayer

Langley Aeronautical Laboratory
Langley Air Force Base, Va.

NATIONAL ADVISORY COMMITTEE
FOR AERONAUTICS

WASHINGTON

February 23, 1949

NACA RM No. L8L07

NATIONAL ADVISORY COMMITTEE FOR AERONAUTICS

RESEARCH MEMORANDUM

ESTIMATION OF LIFT AND DRAG OF AIRFOILS AT NEAR SONIC SPEEDS AND IN THE PRESENCE OF DETACHED SHOCK WAVES

By John P. Mayer

SUMMARY

A semiempirical method of estimating the forces on airfoils at near sonic speeds and in the presence of detached shock waves is presented. Fairly good agreement with the trend of existing experimental data is found at Mach numbers from 0.95 to 2.3 for sharp-nose airfoils at speeds and angles of attack above those at which shock detachment occurs and for blunt-nose airfoils where shock waves always are detached. Computed values of the forces on two-dimensional wings are in good agreement with wind-tunnel data on wings of various plan forms and aspect ratios at high angles of attack. The approximate method is in agreement with the Von Kármán transonic similarity rules for Mach numbers near unity.

INTRODUCTION

Since supersonic airplanes and missiles, in some phases of flight, must operate in regions of detached shock waves, the problem of the forces that may be developed under such conditions is becoming increasingly important. In reference 1 an estimation was made of the limit forces on airfoils associated with detached shock waves at supersonic speeds. The semiempirical method of estimating the limit forces was based on an empirical limit negative pressure coefficient and the maximum positive pressure coefficient attainable behind a normal shock wave. In general, the calculated results agreed well with experimental results at high angles of attack. An extension of the semiempirical method is presented in the present paper to include all speeds and angles of attack where detached shock waves are present and comparisons are made with existing experimental data.

SYMBOLS

A	aspect ratio
c	section chord
c_c	section chord-force coefficient (Chord force/qc)

c_{d_p}	section pressure-drag coefficient (Pressure drag/qc) or $(c_n \sin \alpha + c_c \cos \alpha)$
c_l	section lift coefficient (Lift/qc) or $(c_n \cos \alpha - c_c \sin \alpha)$
$c_{m_{LE}}$	section pitching-moment coefficient about leading edge (Pitching moment/qc^2)
$c_{m_{c/4}}$	section pitching-moment coefficient about quarter-chord point
c_n	section normal-force coefficient (Normal force/qc)
d	section drag
l	section lift
M	Mach number
p	static pressure
P	pressure coefficient $\left(\frac{p - p_o}{q_o}\right)$
q	dynamic pressure $\left(\frac{1}{2} \rho V^2\right)$
t	maximum airfoil thickness
t/c	thickness ratio
V	stream velocity
x	longitudinal distance along chord
y	lateral distance from chord
α	angle of attack
δ_F	flap deflection
γ	ratio of specific heats, taken as 1.40 for air
ρ	stream density
ϕ	angle between tangent to airfoil surface and free-stream direction

[redacted]

Subscripts:

1	forwardly inclined surface
2	rearwardly inclined surface
lim	limit
max	maximum
o	free stream
U	upper surface
L	lower surface

METHOD OF ESTIMATING FORCES

The method for estimating the forces on airfoils at near sonic speeds and in the presence of detached shock waves is based on the maximum pressure coefficients attainable on airfoils in conjunction with certain arbitrary assumptions. In reference 1 an empirical limit negative pressure coefficient was presented, the equation of which was found to be

$$P_{lim} = -\frac{1}{M_o^2} \tag{1}$$

The maximum positive pressure coefficient used is the pressure coefficient corresponding to the total pressure. For subsonic flow, the maximum positive pressure coefficient is

$$P_{max} = \frac{2}{\gamma M_o^2}\left\{\left[1 + \left(\frac{\gamma - 1}{2}\right)M_o^2\right]^{\frac{\gamma}{\gamma-1}} - 1\right\} \tag{2a}$$

In supersonic flow the maximum positive pressure coefficient behind a normal shock wave is

$$P_{max} = \frac{2}{\gamma M_o^2}\left\{\left[\frac{\gamma + 1}{2\gamma M_o^2 - (\gamma - 1)}\right]^{\frac{1}{\gamma-1}}\left[\left(\frac{\gamma + 1}{2}\right)M_o^2\right]^{\frac{\gamma}{\gamma-1}} - 1\right\} \tag{2b}$$

[redacted]

The variation of the limit negative pressure coefficient P_L and the maximum positive pressure coefficient P_{max} with Mach number for Mach numbers greater than 1 is shown in figure 1.

In supersonic flow, at certain angles of attack and speeds, the shock wave is curved and detached from the nose of the airfoil and a region of subsonic flow exists behind the shock wave as is shown in figure 2. The average normal force on an element of forwardly inclined surface is assumed to be equal to the product of the maximum positive pressure coefficient and the sine of the angle between the free-stream direction and the airfoil surface

$$P_1 = P_{max} \sin \phi_1 \tag{3}$$

It is known that, when mixed flow fields are present, sonic velocity is reached on wedges at the shoulder. (See references 2 and 3.) Therefore, for sharp-nose airfoils at high angles of attack, it is assumed that the sonic lines initiate from the leading and trailing edges of the airfoil, as is shown in figure 2(a). For round-nose airfoils and sharp-edge airfoils at low angles of attack it is assumed that the sonic lines initiate from the point on the airfoil surface where the angle between the free-stream direction and the tangent at the airfoil surface is zero. (See figs. 2(b) and 2(c).) The average normal force on an element of a rearwardly inclined surface is then assumed to be given by the well-known Prandtl-Meyer expansion with the static pressure at the sonic line set equal to the free-stream static pressure. It can be shown that the pressure coefficient corresponding to the Prandtl-Meyer relation may be given for small angles as

$$\left.\begin{aligned} P_2 &= -\frac{3^{2/3}}{M_o^2}\left(\frac{2}{\gamma + 1}\right)^{1/3} \phi_2^{\,2/3} \\ \text{or} \\ P_2 &= -\frac{1.957}{M_o^2}\,\phi_2^{\,2/3} \end{aligned}\right\} \tag{4}$$

[redacted]

With the previous simplifying assumptions, the following approximate equations for the normal-force, chord-force, and moment coefficients are obtained:

$$c_n = P_{max}\left[\int \sin \phi_U d(x/c) + \int \sin \phi_L d(x/c)\right] + \frac{1.957}{M_o^2}\left[\int \phi_U^{2/3} d(x/c) + \int \phi_L^{2/3} d(x/c)\right] \quad (5)$$

$$c_c = P_{max}\left[\int \sin \phi_U d(y/c) + \int \sin \phi_L d(y/c)\right] - \frac{1.957}{M_o^2}\left[\int \phi_U^{2/3} d(y/c) + \int \phi_L^{2/3} d(y/c)\right] \quad (6)$$

$$c_{m_{LE}} = P_{max}\left[\int \sin \phi_U (x/c) d(x/c) + \int \sin \phi_L (x/c) d(x/c)\right] - \frac{1.957}{M_o^2}\left[\int \phi_U^{2/3} (x/c) d(x/c) + \int \phi_L^{2/3} (x/c) d(x/c)\right] \quad (7)$$

$$c_{m_{c/4}} = P_{max}\left[\int \sin \phi_U \left(\frac{x}{c} - 0.25\right) d(x/c) + \int \sin \phi_L \left(\frac{x}{c} - 0.25\right) d(x/c)\right] - \frac{1.957}{M_o^2}\left[\int \phi_U^{2/3} \left(\frac{x}{c} - 0.25\right) d(x/c) + \int \phi_L^{2/3} \left(\frac{x}{c} - 0.25\right) d(x/c)\right] \quad (8)$$

In using equation (4) the flow is expanded only until the pressures reach the empirical limit pressure coefficient given in equation (1). A graphical representation of the Prandtl-Meyer relation and equation (4) is presented in figure 3 from which the pressure coefficient P_2 may be found if the free-stream Mach number M_o and the angle of expansion ϕ_2 are given. It may be seen in figure 3 that in using equation (4) instead of the exact Prandtl-Meyer relation, the error is small up to the angle

for limit pressure. Figures 1 and 3, together with the geometric properties of an airfoil, may then be used to approximate the lift and drag coefficients associated with detached shock waves.

APPLICATION AND COMPARISONS

Comparisons between the test results of reference 4, for a rectangular wing having circular-arc airfoil sections, and the calculated force coefficients obtained using the approximate formula given previously are shown in figure 4 for Mach numbers of 1.55 and 2.32. Shown in figure 4, in addition to the calculated force coefficients at angles of attack above the point of shock detachment, are the theoretical angle of attack where the shock detaches from the leading edge of the airfoil and the exact theoretical two-dimensional lift and drag curves for the airfoil up to the angle of shock detachment. It can be seen from figure 4 that, although the equations from which the calculated lift and drag coefficients were obtained are based on a two-dimensional analysis, the results show fairly good agreement with the trend of the three-dimensional wind-tunnel data at angles of attack above the angle of shock detachment even at aspect ratios as low as 1.7. It may be noted that at the angle of shock detachment the calculated lift and drag coefficients are close to the lift and drag coefficients obtained by using the more exact shock-expansion theory (reference 5). For these particular cases the estimated value is within 10 percent of the value obtained using the more exact theory.

Reference 4 also includes results from wind-tunnel tests on wing models of triangular, sweptback, and trapezoidal plan forms with aspect ratios from 1.37 to 4.06. Presented in figure 5 are comparisons between the test results of reference 4 for four wing plan forms with the lift and drag coefficients obtained from equations (5) and (6). It can be seen that the results show fairly good agreement with experiment at high angles of attack.

Comparisons between calculated lift and drag coefficients and experimental two-dimensional data of reference 6 for detached shock conditions are presented in figure 6 for a circular-arc airfoil section at Mach numbers of 1.85 and 2.13. In general, the results show fairly good agreement with the trend of the test data at angles of attack where the shock is detached from the airfoil. At a Mach number of 2.13, however, the slope of the experimental lift curve does not tend to decrease at high angles of attack as does the slope of the calculated lift curve.

Shown in figure 7 are comparisons of the moment coefficients at the leading edge calculated by the approximate method and the experimental moment coefficients for the 10-percent circular-arc airfoil sections of reference 6 for Mach numbers of 1.85 and 2.13. The calculated results

are in fair agreement with the trend of the experimental data and it may be seen that, for these particular cases, the calculated moment coefficients at the point of shock detachment are near those calculated by the more exact shock-expansion two-dimensional theory.

Reference 7 presents results of tests made at supersonic speeds of several subsonic airfoil sections where shock waves always would be detached from the leading edges. Comparisons between the test results of reference 7 and the estimated lift and drag coefficients based on the previous assumptions are shown in figure 8 for three of the blunt-nose airfoils tested at a Mach number of 1.47. Comparisons between the experimental and estimated results for a faired circular cylinder having a thickness ratio of 14 percent are shown in figure 8(a). Shown in figures 8(b) and 8(c) are comparisons for Göttingen airfoils numbers 622 and 623 which have thickness ratios of 8 and 12 percent, respectively. It can be seen that, in general, the estimated lift and drag coefficients agree fairly well with the trend of the experimental lift and drag coefficients.

An application of the approximate method at Mach numbers close to $M = 1.0$ is shown in figure 9 where comparisons are made between the calculated force coefficients for a 12-percent circular-arc airfoil section and some unpublished tests of a semispan rectangular wing having 12-percent circular-arc airfoil sections and an aspect ratio of 5.30. The tests were made in the Southern California Cooperative Wind Tunnel by the "bump" method at a Reynolds number of about 430,000. It may be noted in figure 9 that comparisons are shown for Mach numbers less than $M = 1.0$. When the shock waves on an airfoil approach the trailing edge the air flow is essentially supersonic and the approximate method should be applicable. For most commonly used airfoils this Mach number at which the flow becomes essentially supersonic is near $M = 0.95$ at low angles of attack. Shown in figure 9 are the approximate shock locations at low angles of attack. As the Mach number increases the shock waves approach the trailing edge and reach the trailing edge at a Mach number near $M = 0.95$, and as the Mach number becomes supersonic a bow wave forms in front of the airfoil. It may be seen from figure 9 that the calculated lift coefficients are in good agreement with the experimental lift coefficients at Mach numbers where the shock waves on the airfoil have approached the trailing edge. The calculated pressure-drag coefficients are in fair agreement with experimental total-drag coefficients. The calculated moment coefficients about the quarter-chord point are overestimated in all cases since the pressure distributions obtained from the approximate formulas differ from the experimental pressure distributions.

Shown in figure 10 are comparisons between measured pressure distributions and those calculated from the approximate formulas for circular-arc airfoil sections at Mach numbers of 1.10 and 1.85. The test results at $M = 1.10$ are from the unpublished tests mentioned previously and the results at a Mach number of 1.85 are from reference 6. In both cases,

[redacted]

detached shock waves are present. It may be seen that at a Mach number of 1.10 the approximate method does not predict the actual pressure distribution. However, the areas of the experimental and the approximate curves are nearly the same. At a Mach number of 1.85 the results are somewhat better, although the measured pressures on the lower surface near the leading edge are necessarily higher than those estimated by the approximate formulas.

An application of the method for estimating forces in the presence of detached shock waves is shown in figure 11 where the calculated lift, drag, and moment coefficients are shown for a 10-percent diamond airfoil with a 25-percent-chord trailing-edge flap at a Mach number of 2.5. Also shown are the theoretical two-dimensional lift, drag, and pitching-moment coefficients below the angle of attack for shock detachment. The estimated increments in lift, drag, and moment coefficients at the point of shock detachment are close to the increments calculated by the more exact two-dimensional theory in this case. It can be seen, in figure 11, that the 10° flap deflection produces higher drag and moment coefficients throughout the angle-of-attack range. However, because of the large chord forces, the lift coefficient of the flapped airfoil is actually less than that for the unflapped airfoil at angles of attack above 45° and, for this particular case, the maximum lift coefficient is changed very little by the use of a flap.

DISCUSSION

In applying the approximate method for estimating the forces on airfoils at near sonic speeds and in the presence of detached shock waves, it must be remembered that the method is semiempirical and based on rough assumptions to the actual flow conditions and that some caution should be used. For instance, pressure distributions computed by the approximate method may be considerably in error. Therefore, calculated moments are questionable and such factors as aerodynamic centers or centers of pressure cannot be estimated by the approximate method. On the other hand, calculated lift and drag coefficients are in fairly good agreement with the trend of available test data. In regard to the calculation of forces on round-nose airfoils, it is known that there will be considerable error in the assumed position of the sonic line and the assumed static pressure at the sonic line. However, for the particular examples given in the present paper, it is believed that the assumption of the position of the sonic line is not too much in error since the position of maximum thickness occurs fairly close to the leading edge of the airfoil. For airfoils having the position of maximum thickness farther rearward, however, the assumption would be more in error at low angles of attack, for the sonic lines would initiate ahead of the assumed point. At higher angles of attack the results might be better.

A closer assumption to the actual conditions would be to assume the sonic line at the point on the airfoil surface where the angle ϕ is equal to the maximum angle through which a supersonic flow may be deflected and to assume a static pressure at the sonic line corresponding to equation (3) for this case. In the actual case, the sonic line probably initiates somewhat ahead of the point on the airfoil where the angle ϕ is equal to the maximum deflection angle. The flow then expands over the airfoil surface but is affected by the reflection of compression waves from the sonic line. (See reference 3.) The use of the approximate equations used in the present paper $\left(P_1 = P_{max}\sin\phi_1 \text{ for forwardly inclined surfaces and } P_2 = -\frac{3^{2/3}}{M_o^2}\left(\frac{2}{\gamma+1}\right)^{1/3}\phi_2^{2/3} \text{ for rearwardly inclined surfaces}\right)$ introduces somewhat compensating factors in regard to actual flow conditions since, in starting the expansion from the point on the airfoil where $\phi = 0^\circ$, the negative pressures are reduced from what they would be by starting the expansion from the point where ϕ is equal to the maximum deflection angle.

In regard to the use of the approximate method at Mach numbers near $M = 1.0$, it can be shown that, for thin symmetrical airfoils at low angles of attack, the lift and drag coefficients obtained from equations (5) and (6) can be expressed as

$$c_l = \frac{1}{M_o^2}\alpha^{2/3}\left(P_{max}M_o^2\alpha^{1/3} + \text{Constant}\right) \tag{9}$$

and

$$c_d = \frac{1}{M_o^2}\left(\frac{t}{c}\right)^{5/3}\left[P_{max}M_o^2\left(\frac{t}{c}\right)^{1/3} + \text{Constant}\right] \tag{10}$$

These equations are in agreement with the transonic similarity laws of Von Kármán. (See references 8 and 9.) From these laws the lift and drag coefficients are expressed as

$$c_l = \frac{1}{M_o^2}\alpha^{2/3}L\left[\frac{\alpha^{1/3}}{\left(\left|1 - M_o^2\right|\right)^{1/2}}\right] \tag{11}$$

and

[redacted]

$$c_d = \frac{1}{M_o^2}\left(\frac{t}{c}\right)^{5/3} D\left[\frac{(t/c)^{1/3}}{\left(|1 - M_o^2|\right)^{1/2}}\right] \qquad (12)$$

In estimating the lift and drag of airfoils at Mach numbers near $M = 1.0$ the approximate method should be used only for Mach numbers and angles of attack where the shock waves on the airfoil have approached the trailing edge. At high subsonic Mach numbers the air flow over the rear portion of an airfoil often separates and the shock wave on the upper surface of the airfoil tends to move forward with increasing angle of attack. Therefore, it might be expected that the lift and drag obtained by the approximate method at high angles of attack in the transonic range would not be as good an estimation as the lift and drag obtained at low angles of attack.

It is of interest to study the conditions under which the shock is detached and the approximate method may be used. Guderley has shown that the transition from an attached to a detached shock wave is not an abrupt change but is a continuous process. (See reference 3.) In reality, even the sharpest wedge or airfoil has a blunt nose and the shock wave has a small region of detachment. However, the problem is a relative one and a strong region of shock detachment must be present before the ordinary methods of treating attached shock waves cease to be useful. At high supersonic Mach numbers and low angles of attack where the shock is bent strongly back the subsonic region of flow on the airfoil is small and perhaps the attached shock methods may be used again with success even for round-nose airfoils. In the present paper, however, the approximate method is for use in estimating the lift and drag of airfoils at supersonic speeds in the presence of relatively strong detached shock waves. In general it is believed that, in the absence of a more exact theoretical solution, the simple method presented will enable a first approximation of the lift and drag of airfoils at high transonic speeds and at supersonic speeds in the presence of detached shock waves.

CONCLUDING REMARKS

A semiempirical method for estimating the forces on airfoils at sonic speeds and at supersonic speeds in the presence of detached shock waves is presented. Fairly good agreement with the trend of existing experimental data is found at Mach numbers from 0.95 to 2.3 for sharp-edge airfoils above the angle of attack for shock detachment, and the calculated results agree fairly well with the trend of the experimental data for blunt-nose airfoils at supersonic speeds where shock waves

always are detached from the leading edge. Computed values of the forces on two-dimensional wings are in good agreement with wind-tunnel data on wings of various plan forms and with aspect ratios as low as 1.7 at high angles of attack.

For airfoils considered in this paper, the estimated force coefficients at the angle of attack where the shock wave detaches from the nose of a sharp-edge airfoil are close to the theoretical two-dimensional force coefficients.

The approximate method presented is in agreement with the Von Kármán transonic similarity rules for Mach numbers near unity.

Langley Aeronautical Laboratory
National Advisory Committee for Aeronautics
Langley Air Force Base, Va.

[redacted]

REFERENCES

1. Mayer, John P.: A Limit Pressure Coefficient and an Estimation of Limit Forces on Airfoils at Supersonic Speeds. NACA RM No. L8F23, 1948.

2. Maccoll, J. W., and Codd, J.: Theoretical Investigations of the Flow around Various Bodies in the Sonic Region of Velocities. British Theoretical Res. Rep. No. 17/45, B.A.R.C. 45/19, Ministry of Supply, Armament Res. Dept., 1945.

3. Guderley, G.: Considerations of the Structure of Mixed Subsonic-Supersonic Flow Patterns. Tech. Rep. No. F-TR-2168-ND, Air Materiel Command (Wright Field), Oct. 1947.

4. Gallagher, James J., and Mueller, James N.: Preliminary Tests to Determine the Maximum Lift of Wings at Supersonic Speeds. NACA RM No. L7J10, 1947.

5. The Staff of the Ames 1- by 3-Foot Supersonic Wind-Tunnel Section: Notes and Tables for Use in the Analysis of Supersonic Flow. NACA TN No. 1428, 1947.

6. Ferri, Antonio: Experimental Results with Airfoils Tested in the High-Speed Tunnel at Guidonia. NACA TM No. 946, 1940.

7. Busemann, A., and Walchner, O.: Profileigenschaften bei Überschallgeschwindigkeit. Forsch. auf dem Geb. des Ingenieurw., Ausg. A, Bd. 4, Heft 2, March/April 1933, pp. 87-92.

8. Von Kármán, Theodore: The Similarity Law of Transonic Flow. Jour. Math. and Phys., vol. XXVI, no. 3, Oct. 1947, pp. 182-190.

9. Kaplan, Carl: On Similarity Rules for Transonic Flows. NACA TN No. 1527, 1948.

[redacted]

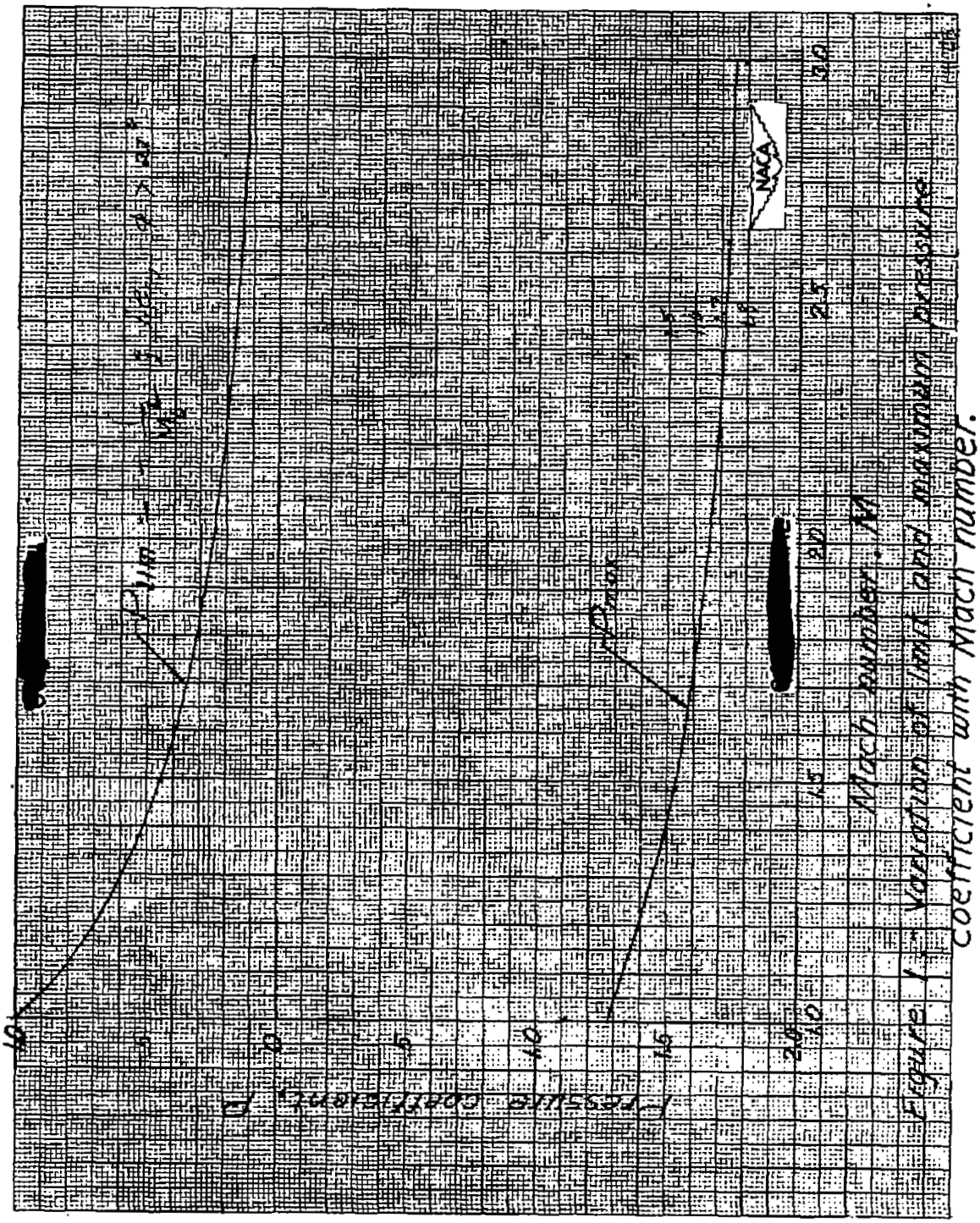

Figure 1.- Variation of limit load maximum pressure coefficient with Mach number.

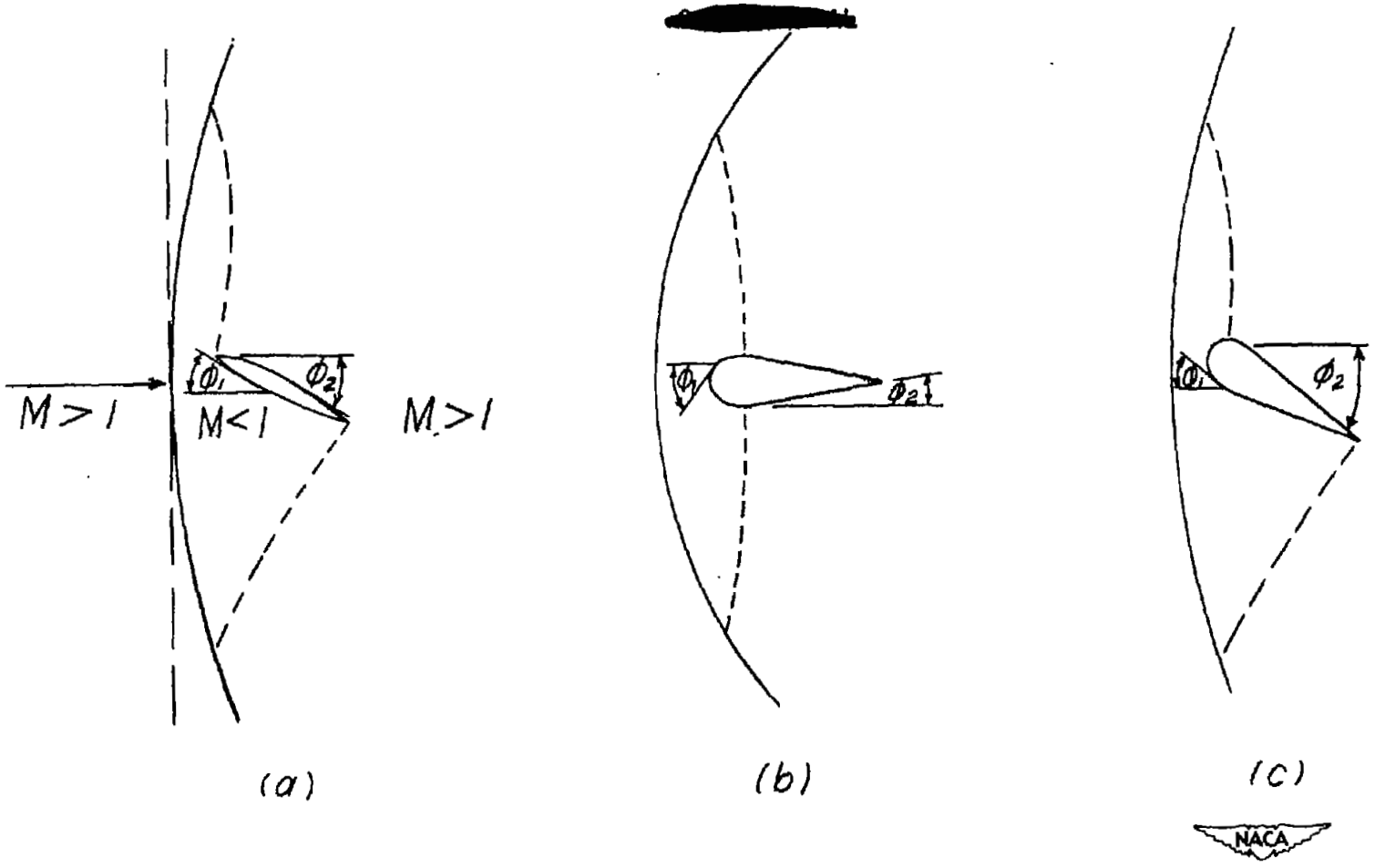

Figure 2.–Airfoils with detached shock waves in supersonic flow.

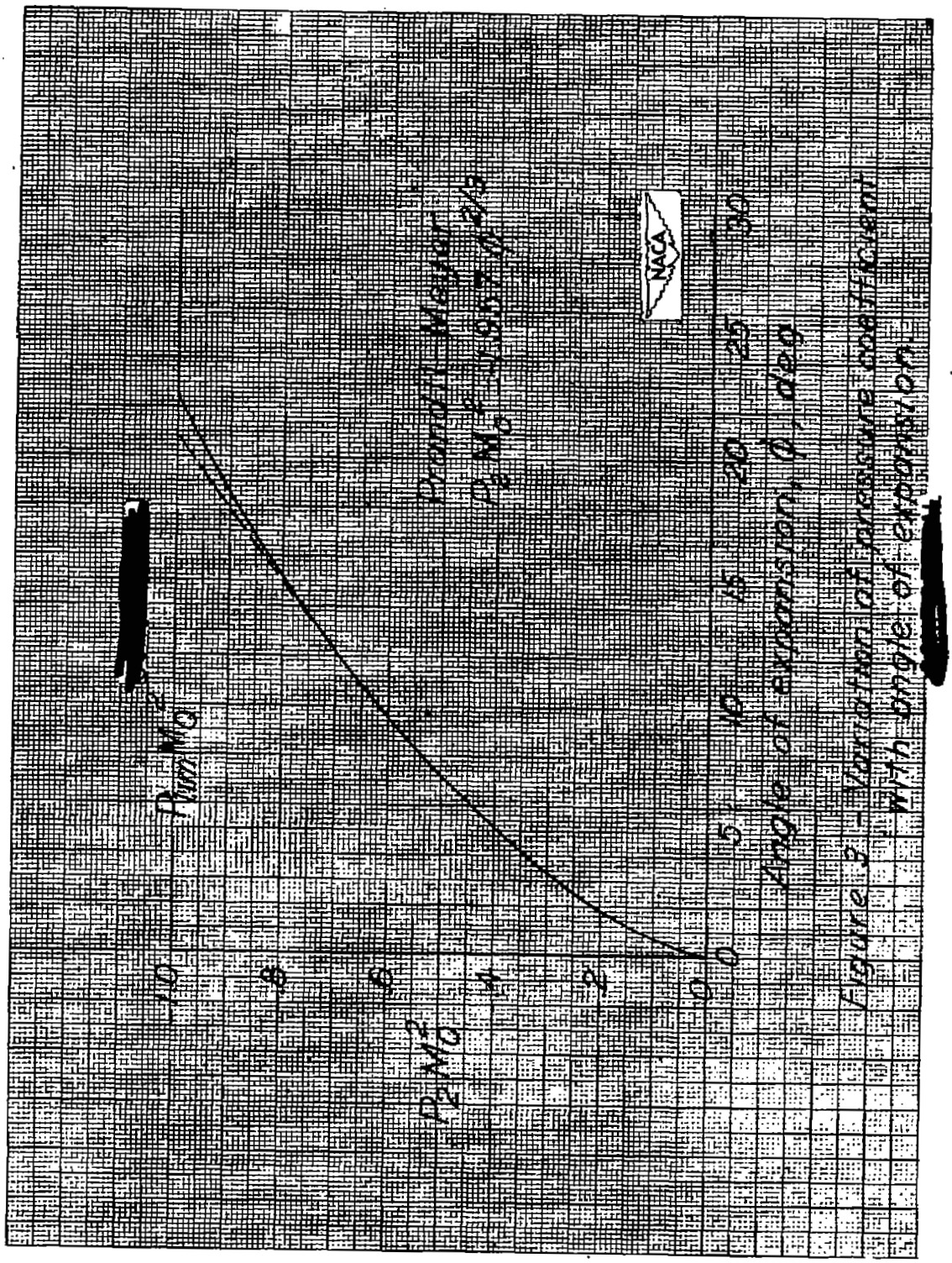

Figure 3.- Variation of pressure coefficient with angle of expansion at various angles of attack.

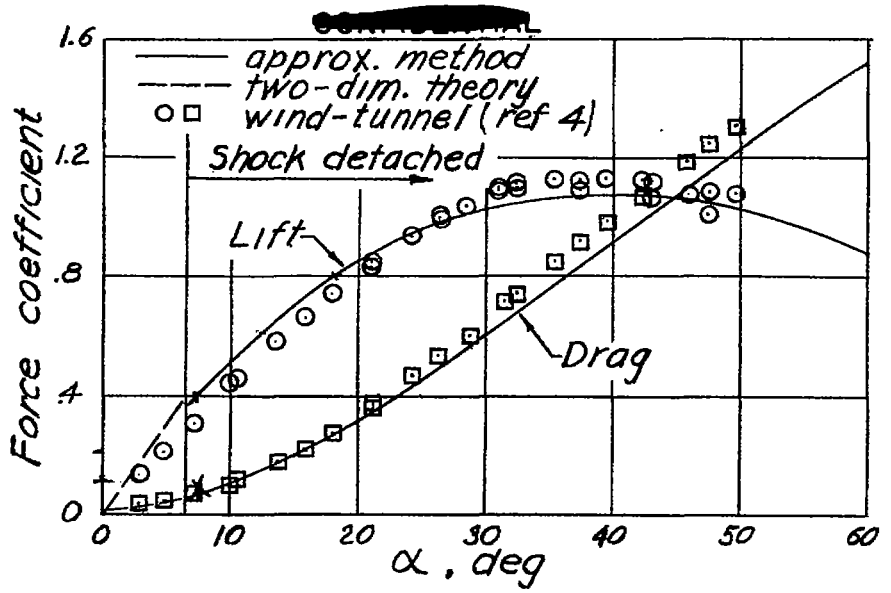

(a) $M = 1.55$; $A = 1.74$; $t/c = 0.06$.

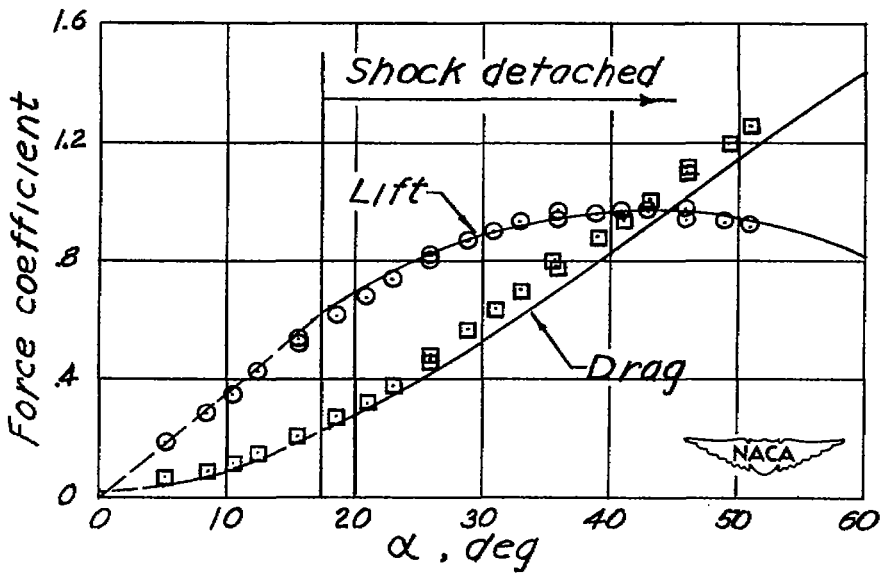

(b) $M = 2.32$; $A = 1.99$; $t/c = 0.09$.

Figure 4.- Comparison between calculated and experimental force coefficients for rectangular wings with biconvex airfoil sections.

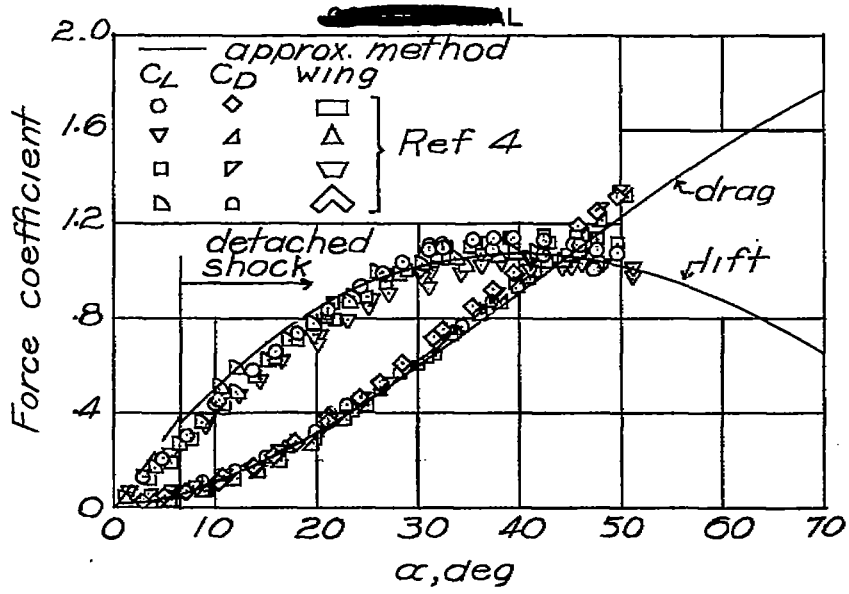

(a) $M = 1.55$.

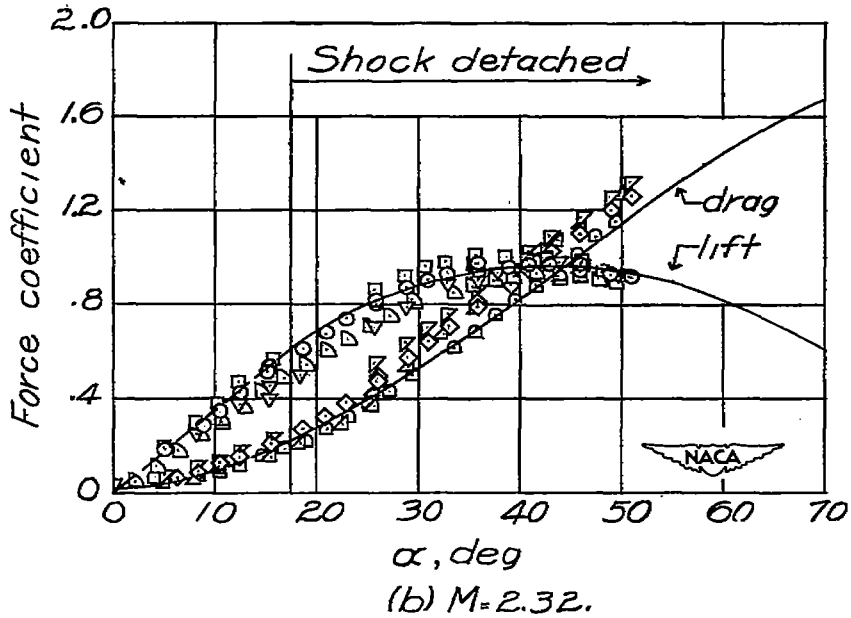

(b) $M = 2.32$.

Figure 5.- Comparison between calculated and experimental force coefficients for various wing plan forms.

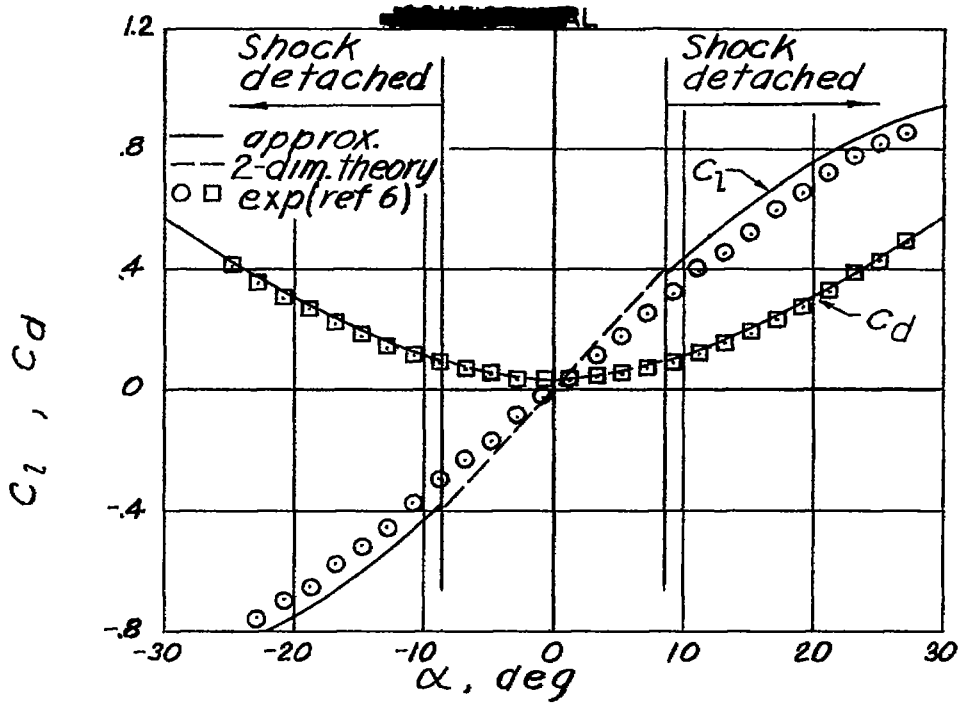

(a) $M = 1.85$; $t/c = 0.10$.

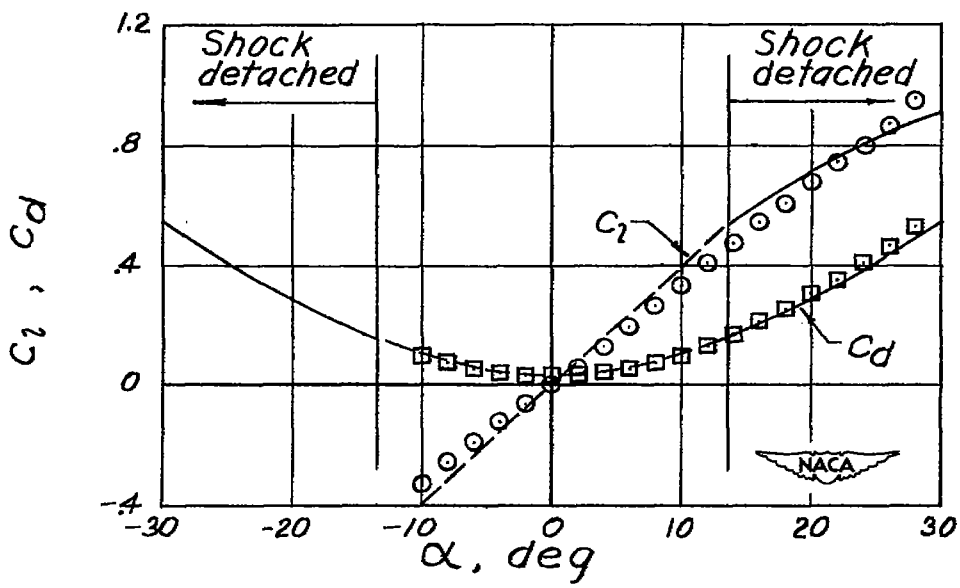

(b) $M = 2.13$; $t/c = 0.10$.

Figure 6.—Comparison between calculated and experimental force coefficients for two-dimensional biconvex airfoil sections.

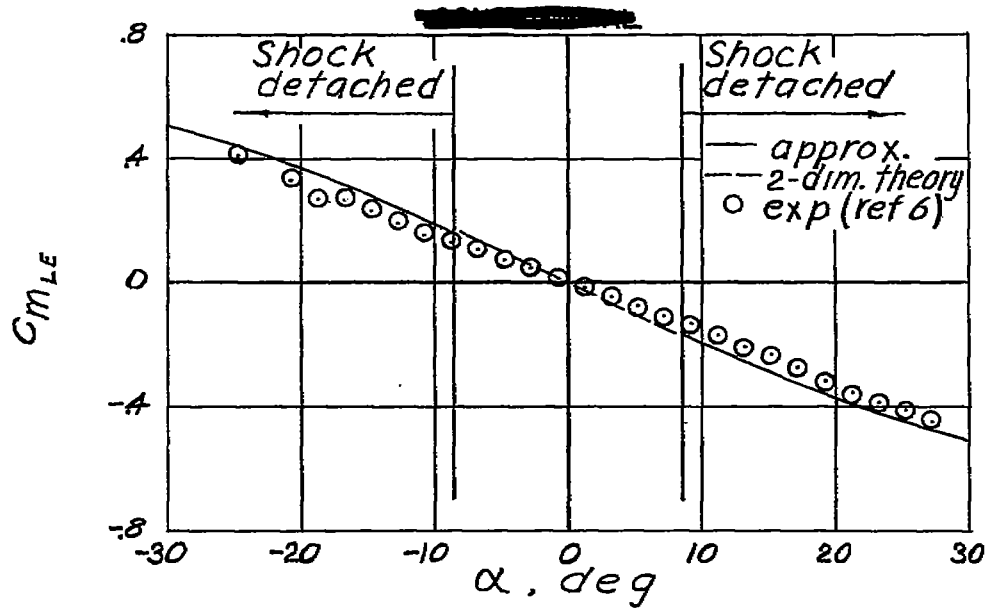

(a) $M = 1.85$; $t/c = 0.10$.

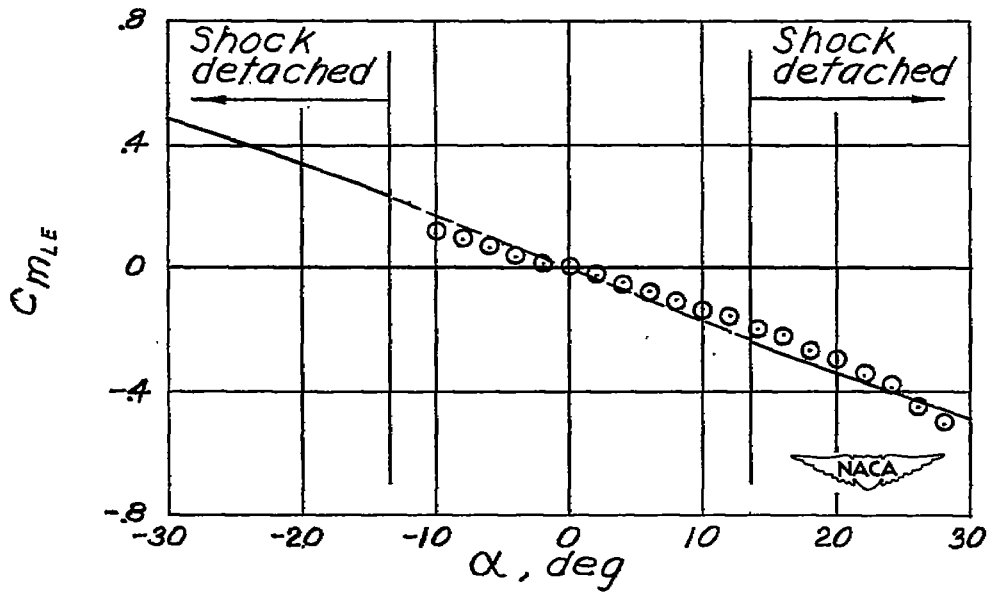

(b) $M = 2.13$; $t/c = 0.10$.

Figure 7.- Comparison between calculated and experimental moment coefficients for biconvex airfoil sections.

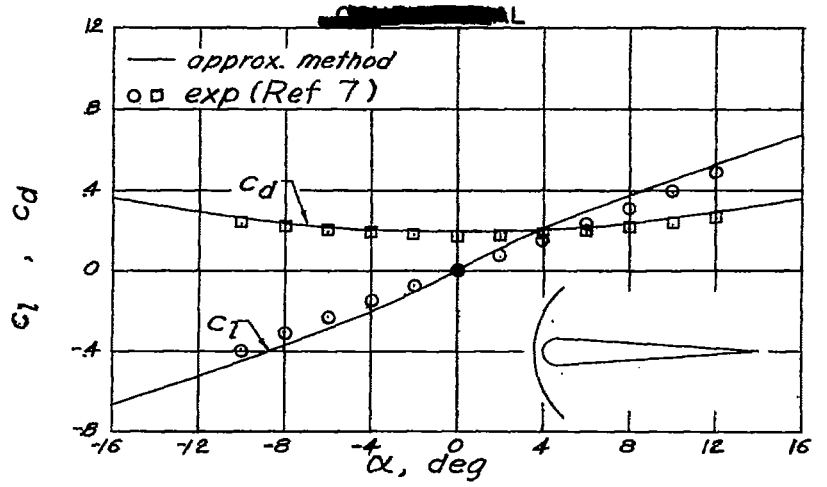

(a) Faired cylinder; $M=1.47$; $t/c=0.14$.

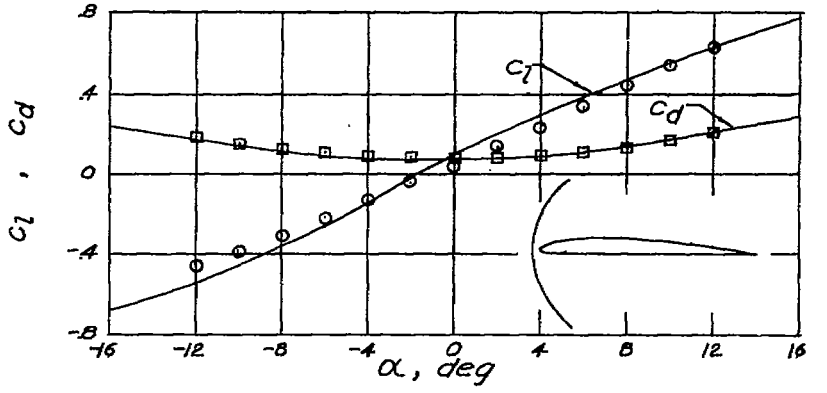

(b) Göttingen 622; $M=1.47$; $t/c=0.08$.

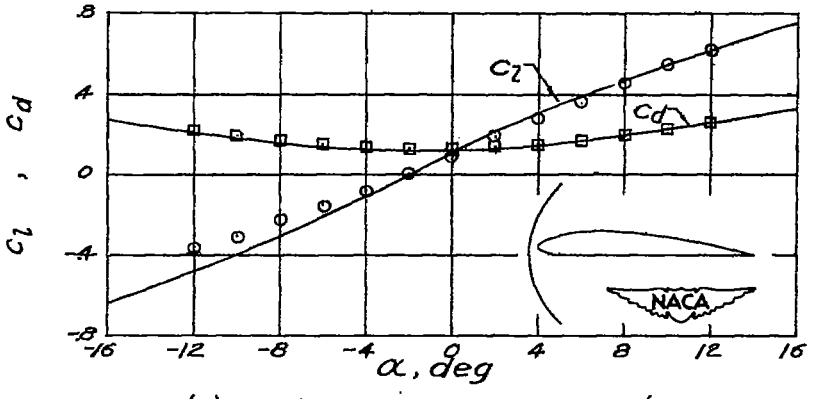

(c) Göttingen 623; $M=1.47$, $t/c=0.12$.

Figure 8.- Comparison between calculated and experimental force coefficients on blunt-nosed airfoils at supersonic speeds.

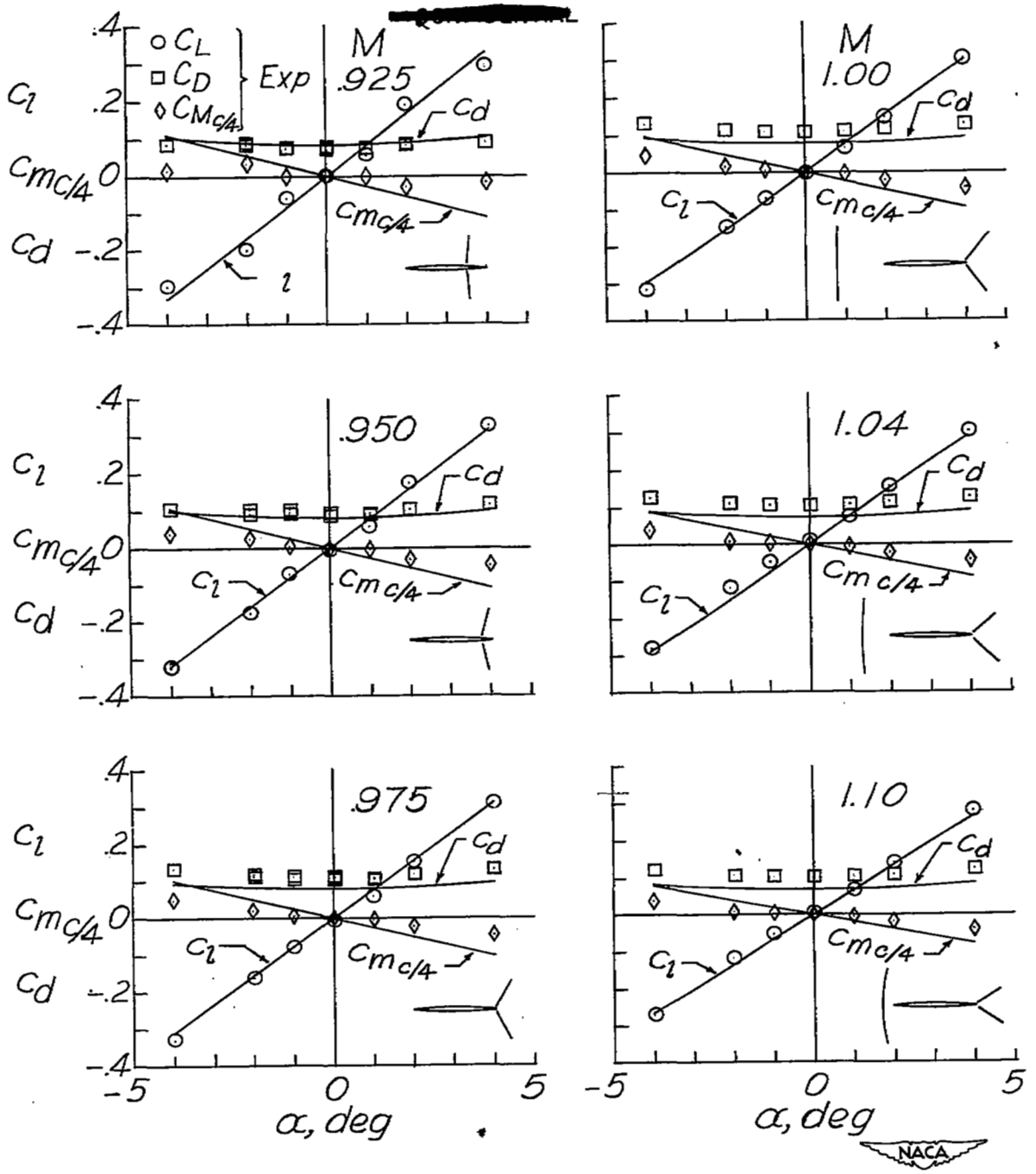

Figure 9.- Comparisons between calculated and experimental force coefficients at transonic speeds.

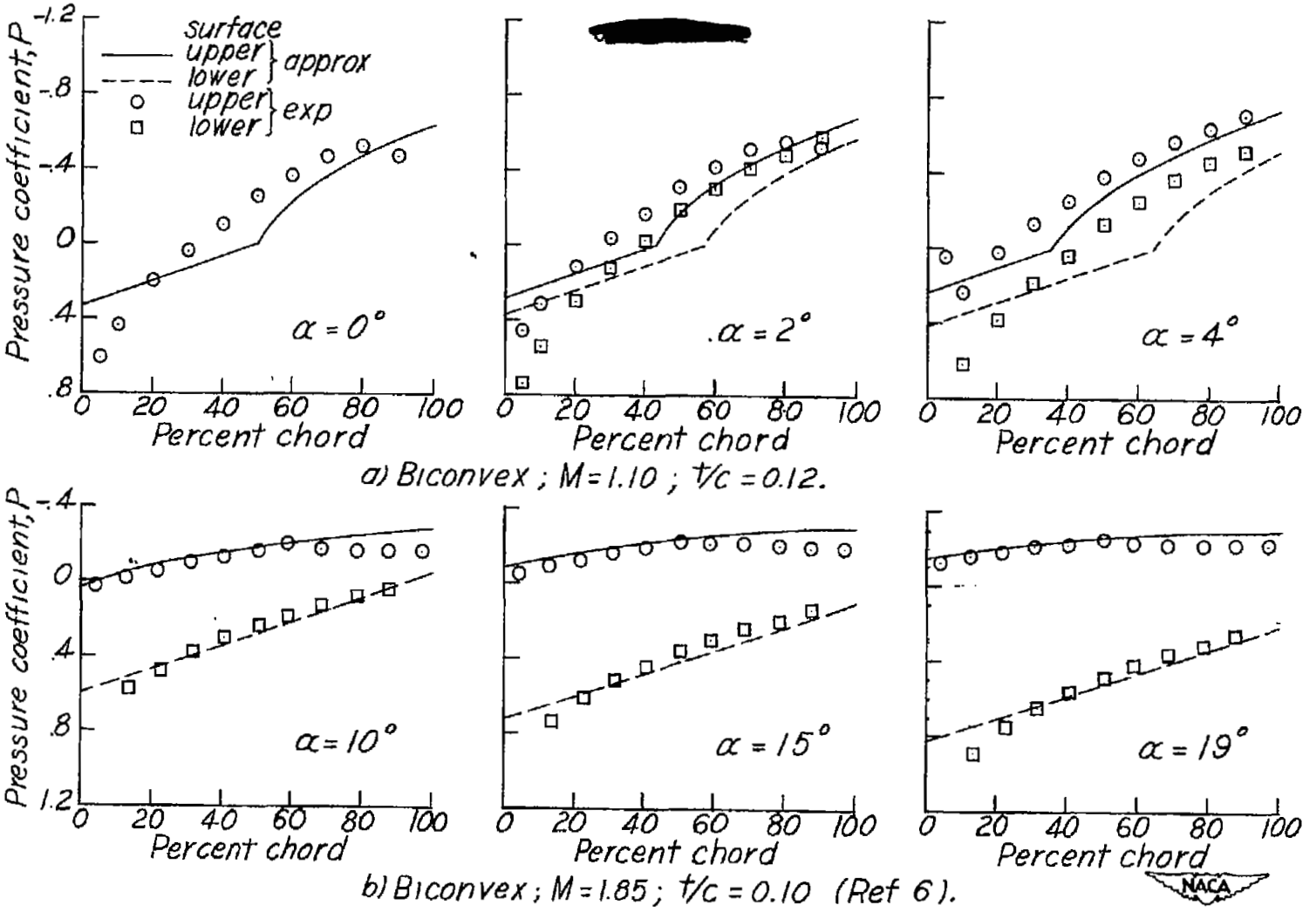

Figure 10.- Comparison between calculated and experimental pressure distributions.

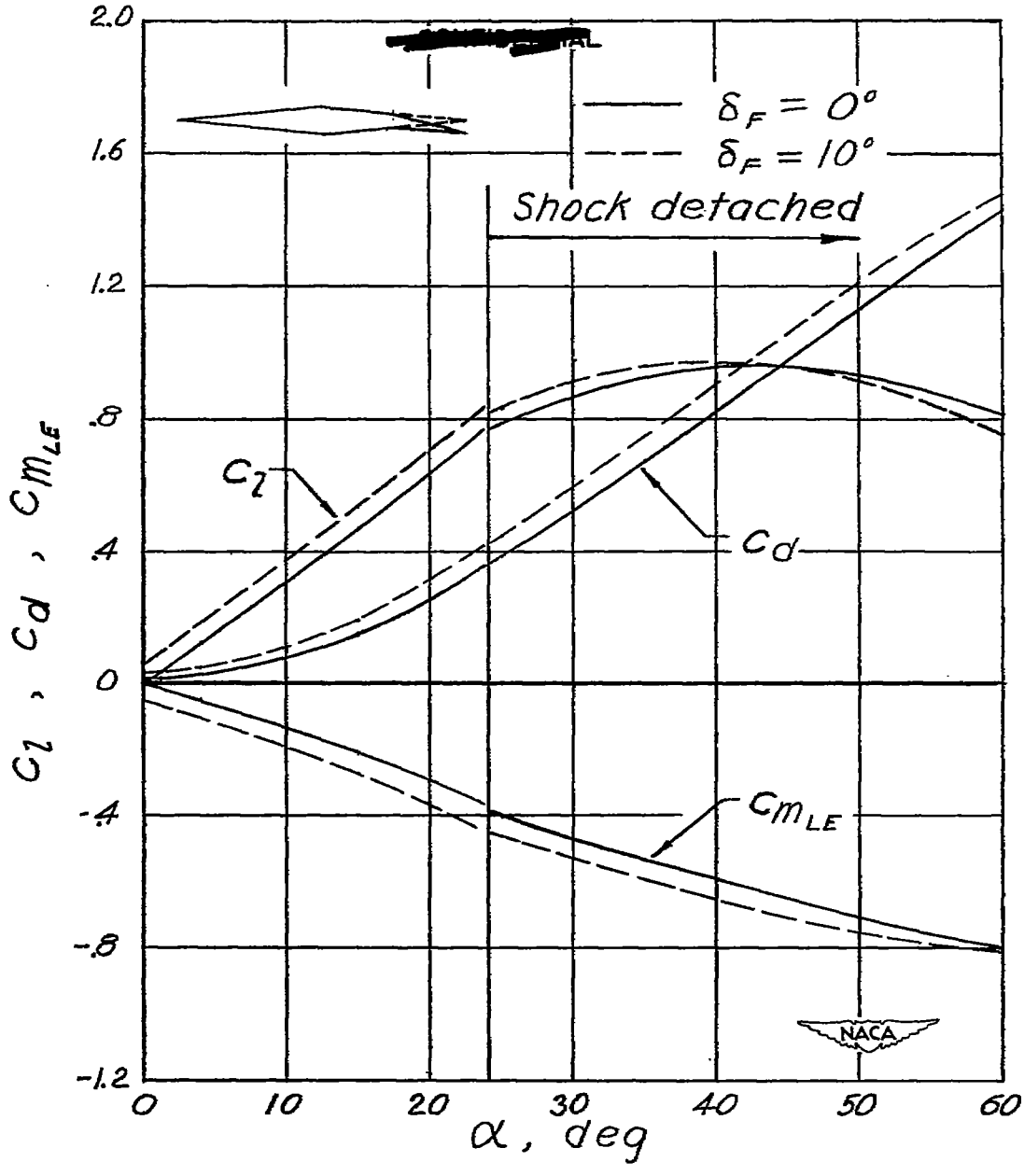

Figure 11.- Effect of a 25-percent-chord flap on the characteristics of a 10-percent symmetrical diamond airfoil at a Mach number of 2.50.